ISSN: 2688-8645

# Study on the Effect of Laser Shock Peening Parameters on the Wear Performance of 55SiMoVA Bearing Steel

Lin Zhong, Wenzi Luo

School of Mechanical Engineering, Southwest Petroleum University, Chengdu, Sichuan, 610000, China

## Abstract

**The wear performance of 55SiMoVA bearing steel under extreme service conditions in oil and gas screw drilling tools is critical to the reliability and operational lifetime of thrust ball bearings. In service, these bearings experience severe friction between the balls and raceways, leading to accelerated wear and even catastrophic failure. Conventional surface modification techniques, such as carburizing, nitriding, shot peening, or surface coatings, provide limited improvements in surface properties and often fail to sustain high-load, high-temperature, and complex lubrication environments. Laser shock peening (LSP) has emerged as an effective surface engineering technique capable of inducing deep compressive residual stresses and forming a hardened surface layer, thereby enhancing both mechanical and tribological performance. In this study, 55SiMoVA steel specimens were treated using LSP with systematically varied process parameters, including impact energies of 4 J, 5 J, and 6 J, and impact numbers of one and two. The effects of these parameters on surface microstructure and mechanical properties were evaluated through surface roughness measurement, microhardness profiling, and X-ray diffraction-based residual stress analysis. To assess tribological behavior, reciprocating linear ball-on-block wear tests were conducted under lubrication with oil-based drilling fluid, simulating realistic service conditions. The results demonstrate that LSP markedly alters the surface and near-surface characteristics of 55SiMoVA steel. The maximum microhardness increase reached 17%, compressive residual stress exceeded 823 MPa, and the hardened layer extended to a depth of 1.3 mm, with a gradual stress gradient from surface to substrate. Single-impact treatments showed limited improvements in friction stability, whereas double-impact treatments significantly stabilized the coefficient of friction and enhanced wear resistance. Among all parameter combinations, the 5 J × 2-impact treatment exhibited the most favorable performance, reducing wear volume by approximately 15% compared to untreated specimens. Microscopic analysis of worn surfaces revealed that untreated samples displayed severe plowing and material spalling, while optimally treated samples exhibited relatively uniform and shallow wear tracks, indicating improved surface integrity. Overall, the study confirms that appropriate selection of LSP parameters can effectively enhance the surface hardness, residual compressive stress, and hardened layer depth of 55SiMoVA bearing steel, thereby significantly improving its wear resistance under lubricated conditions. These findings not only provide a practical surface engineering strategy for extending the operational lifetime of thrust ball bearings in screw drilling tools subjected to extreme and complex conditions, but also contribute to a broader understanding of LSP-induced surface modifications for high-strength alloy steels. The insights gained from this work offer valuable guidance for optimizing LSP processing parameters to achieve superior tribological performance and mechanical reliability in demanding industrial applications.**

ISSN: 2688-8645

## Keywords

**Laser Shock Peening; Impact Energy; Impact Number; 55SiMoVA Bearing Steel; Wear Resistance; Hardened Layer Depth; Oil-based Drilling Fluid.**

## 1. Introduction

55SiMoVA is a bearing steel characterized by high strength, excellent impact toughness, superior wear resistance, and outstanding fatigue performance. Owing to these advantages, it is widely employed in the manufacture of heavy-duty impact-resistant bearings, particularly thrust ball bearings used in oil and gas screw drilling tools. However, under low-speed and heavy-load operating conditions with drilling fluid lubrication, the bearing assemblies in screw drilling tools are subjected to extremely high loads. This often leads to severe friction between the rolling elements and the inner and outer raceways, resulting in pronounced wear or even catastrophic fracture of the balls and raceways. Field failure statistics of oil and gas screw drilling tools indicate that thrust ball bearings are among the most failure-prone components in these systems [1,2], and their wear performance plays a decisive role in determining the service life of screw drilling tools. Therefore, enhancing the tribological performance at the contact interfaces between the balls and raceways is of critical importance for extending the operational lifetime of screw drilling tools.

At present, efforts to improve the wear resistance of thrust ball bearings in oil and gas screw drilling tools have mainly focused on investigations into bearing mechanics and kinematics, structural optimization, and material modification. Yu et al. [3] reported that thrust ball bearings with circular surface textures exhibited superior load-carrying capacity and frictional performance compared with untextured bearings, achieving improvements of approximately 28.8% and 18.9%, respectively, while triangular textures demonstrated the most significant temperature reduction, decreasing by about 1.93%. Han et al. [4] designed a deep-cavity hollow tapered roller structure, which effectively alleviated stress concentration at the bearing ends and mitigated premature fatigue failure of the bearing assembly. Sexton et al. [5] experimentally investigated the reliability of polycrystalline diamond bearings in oil and gas screw drilling tools, demonstrating their exceptional wear resistance and their capability to significantly prolong tool service life. Nevertheless, as drilling environments become increasingly harsh, reliance solely on structural optimization of bearing assemblies has proven insufficient to meet performance demands. Although polycrystalline diamond bearings offer outstanding wear resistance, their widespread application is constrained by high manufacturing complexity, stringent process control requirements, and prohibitive costs. Consequently, there is an urgent need for transformative and cost-effective approaches to enhance the tribological performance of thrust ball bearings in oil and gas screw drilling tools.

Laser shock peening (LSP), as an advanced surface strengthening technique, induces high-amplitude plastic deformation in the near-surface region of materials, leading to significant hardness enhancement and the introduction of beneficial residual compressive stresses. These effects collectively contribute to improved wear resistance and fatigue performance [6,7,8,9,10,11,12]. In recent years, extensive studies have confirmed the effectiveness of LSP in tailoring the tribological behavior of metallic materials. Zhou et al. [13] demonstrated that LSP markedly reduced the friction coefficient and wear volume of Ti-6Al-4V alloy, attributing the improvement to the synergistic effects of residual compressive stress and microstructural refinement. Park et al. [14] highlighted the critical role of laser energy in the formation of the strengthened layer in Al–Si alloys, noting that higher laser energy promotes surface densification and enhances frictional performance. Nataraj et al. [15] further revealed that laser energy density plays a decisive role in dislocation evolution, crystallographic texture reconstruction, and stress field development in Ti–2.5Cu alloy. In addition to laser energy, the

ISSN: 2688-8645

number of laser shocks is another key parameter governing the effectiveness of LSP. He et al. [16] reported that a moderate increase in shock number enhanced the magnitude of residual compressive stress and the depth of the strengthened layer in GCr15 bearing steel, thereby improving its wear resistance. Similarly, Muthukumaran et al. [17] demonstrated that multiple laser impacts on EN25 low-alloy steel resulted in a deeper strengthened layer, optimized stress distribution, and significantly improved mechanical performance and microstructural stability. Collectively, these studies indicate that LSP parameters, particularly energy density and shock number, play a critical role in determining surface strengthening effectiveness and tribological behavior. However, investigations into the application of LSP for improving the wear performance of 55SiMoVA bearing steel remain relatively limited.

In this study, the effects of laser shock peening parameters on the wear performance of 55SiMoVA bearing steel are systematically investigated. The influence of LSP parameters on key surface and subsurface characteristics, including residual compressive stress, microhardness, hardened layer depth, and surface roughness, is examined. Furthermore, wear behavior under oil-based drilling fluid lubrication is evaluated using a ball-on-block tribological configuration. Based on the experimental results, optimal LSP parameter combinations are identified, and the underlying wear mechanisms are elucidated. The findings of this work provide a surface strengthening strategy and technical support for further enhancing the wear resistance of thrust ball bearings in screw drilling tools operating under extremely harsh service conditions.

## 2. Experiments

### 2.1. Laser Shock Peening Procedure

In this study, 55SiMoVA bearing steel was selected as the experimental material. The specimens were machined from an 8 mm-thick steel plate that had undergone heat treatment and grinding by Henan Yuhua Bearing Co., Ltd. The heat treatment process consisted of quenching at 870 °C for 120 min, followed by tempering at 200 °C for 60 min. After tempering, the hardness of the specimens reached 631.5 HV.

The chemical composition and mechanical properties of the 55SiMoVA bearing steel at room temperature are summarized in Table 1.

**Table 1.** Chemical composition and mechanical properties of 55SiMoVA bearing steel

| | | Chemical composition | | | | | | | Mechanical properties | | | |
|---|---|---|---|---|---|---|---|---|---|---|---|---|
| Element | | C | Si | Mn | Mo | V | Others | | $\sigma_b$(MPa) | $\sigma_s$(MPa) | υ | E(MPa) |
| Percentage(wt%) | | 0.52 | 0.90 | 0.30 | 0.40 | 0.15 | 0.365 | | 2332 | 1940 | 0.25 | 200900 |

The laser shock peening experiments were conducted using an infrared nanosecond pulsed laser system (YD60-R200B, Xi'an Tianruida Optoelectronic Technology Co., Ltd.). The laser parameters were as follows: wavelength of 1064 nm, pulse duration of 18 ns, repetition frequency of 2 Hz, and spot diameter of 3 mm.

Two LSP treatment strategies were employed in this study. In the first scheme, the laser energy was varied from 4 J to 6 J while keeping all other parameters constant. In the second scheme, the laser energy was fixed, and the number of laser shocks was adjusted to one and two impacts, with the remaining parameters unchanged. In all cases, the spot overlap ratio was maintained at 50%. The detailed LSP parameters for different specimens are listed in Table 2.

The LSP-treated area was a centrally distributed square region of 10 mm × 10 mm on a steel plate measuring 20 mm × 20 mm. The schematic illustration of the LSP process is shown in Fig.

ISSN: 2688-8645

1(a). A deionized water layer with a thickness of 1–2 mm was employed as the confining layer, while a 0.12 mm-thick special aluminum foil was used as the sacrificial absorbing layer. This configuration effectively protected the substrate from laser ablation while enhancing laser energy absorption. The laser scanning path adopted during processing is illustrated in Fig. 1(b).

## 2.2. Surface Roughness Characterization

The surface morphology of the specimens before and after LSP treatment was characterized using a white light interferometer (ContourX-500, Bruker). Surface scanning was initiated from the central region of the specimen and performed along a zigzag trajectory to obtain a rectangular topography map with dimensions of 5 mm × 5 mm. Surface roughness parameters were recorded to quantitatively evaluate the surface morphological changes induced by laser shock peening.

**Table 2.** Process parameters of laser shock peening (LSP)

| Specimen ID | Number of impacts | Laser energy（J） |
|---|---|---|
| Specimen 0 | 0 | 0 |
| Specimen 1 | 1 | 4 |
| Specimen 2 | 1 | 5 |
| Specimen 3 | 1 | 6 |
| Specimen 4 | 2 | 4 |
| Specimen 5 | 2 | 5 |
| Specimen 6 | 2 | 6 |

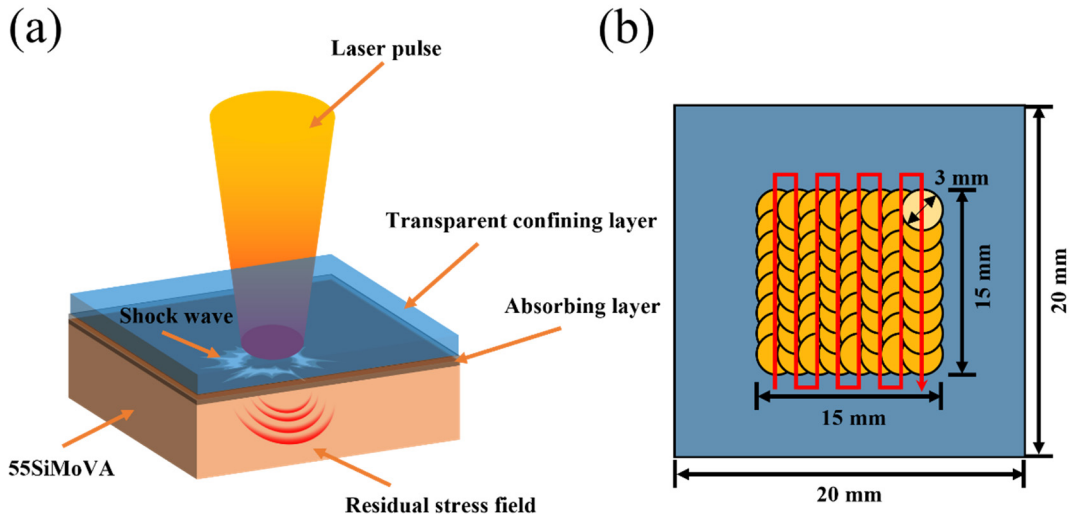


**Fig 1.** Schematic diagram of the LSP experimental principle (a) and the impact strengthening path and region (b)

## 2.3. Microhardness and Residual Stress Measurements

Figure 2 illustrates the measurement locations and regions for microhardness and residual stress characterization. The surface and cross-sectional microhardness distributions of the specimens before and after LSP treatment were measured using an automatic microhardness tester (HXD-2000TM/LCD, Shanghai Tuanjie Instrument Manufacturing Co., Ltd.). A load of 9.807 N was applied with a dwell time of 10 s. As shown in Fig. 2(a), cross-sectional microhardness measurements were initiated at a depth of 150 μm below the treated surface and conducted at intervals of 50 μm down to a depth of 1 mm. To ensure data reliability, three measurements were performed at each depth, with the spacing between adjacent indentations set to three times the diagonal length of the indentation (approximately 150 μm).

ISSN: 2688-8645

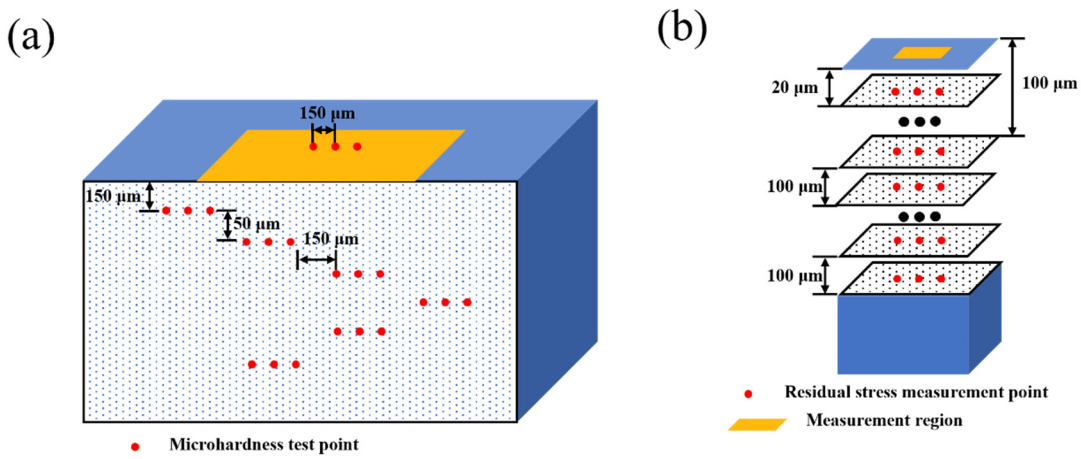


**Fig 2.** Characterization methods of (a) microhardness and (b) residual stress

Residual stress distributions along the depth direction were measured using an X-ray residual stress analyzer (μ-X360s, Pulstec). A Cr-K characteristic X-ray source was employed with a tube voltage of 26 kV and a tube current of 6 mA. The diffraction plane selected was the (211) plane, with a tilt angle range from 0° to 45° and eight measurement points. Material removal for depth profiling was carried out using an electrolytic polishing method with a 3.5% saturated sodium chloride solution as the electrolyte. As shown in Fig. 2(b), residual stress measurements were performed at intervals of 20 μm from the surface to a depth of 100 μm, followed by measurements at 100 μm intervals for greater depths.

## 2.4. Tribological Tests

The tribological performance of the specimens was evaluated under oil-based drilling fluid lubrication using a variable-load friction and wear testing system (UMT-TriboLab, Bruker). The friction configuration was a linear reciprocating sliding motion in a ball-on-flat contact mode. The counterbody was a GCr15 steel ball with a diameter of 6.35 mm, surface roughness of 0.2 μm, and hardness of 61–65 HRC. The test parameters are summarized in Table 3. The specimen dimensions were 20 mm × 20 mm × 8 mm.

Prior to each test, both the steel ball and the specimen were ultrasonically cleaned in acetone, followed by a second ultrasonic cleaning in ethanol, and then dried. All friction and wear tests were conducted under oil-based drilling fluid lubrication and repeated three times to ensure repeatability and consistency of the results.

After testing, the wear morphology, cross-sectional wear profiles, wear volume, wear width, and maximum wear depth were measured using a white light interferometer (ContourX-500, Bruker). To accurately compare wear volumes before and after testing, three-dimensional surface morphologies were characterized at the designated wear locations prior to and following the tribological experiments. In addition, the worn surfaces of the specimens and counterbodies were examined using a scanning electron microscope (Sigma 300, Zeiss) to investigate the wear mechanisms.

**Table 3.** Parameters for the friction and wear tests

| Parameters | Values |
|---|---|
| Load | 200 N |
| Stroke | 5 mm |
| Time | 120 min |
| **Speed** | 3 Hz |
| Temperature | 23 ℃ |

ISSN: 2688-8645

# 3. Results and Discussion

## 3.1. Surface Roughness Analysis

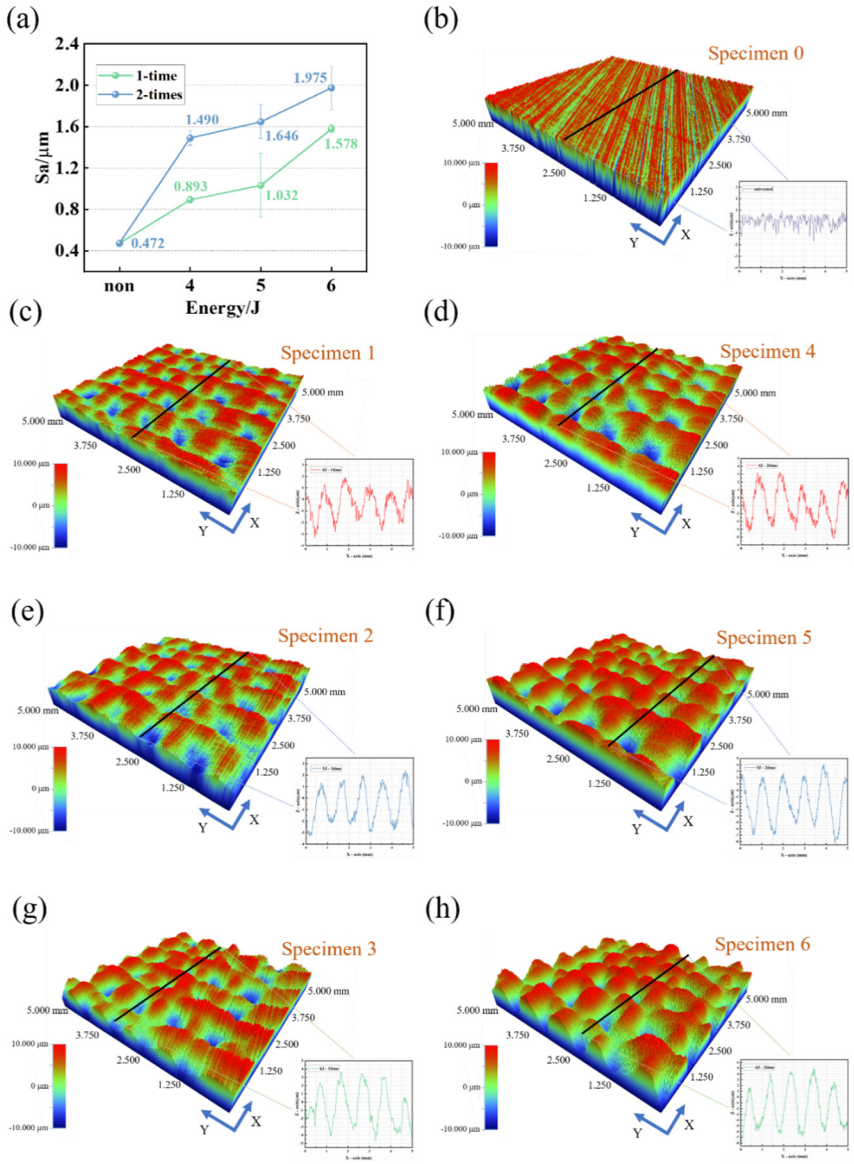


**Fig 3.** Surface roughness of specimens under LSP process parameters: (a) roughness measurement; (b) untreated specimen; (c–h) 3D surface topography and roughness comparison of LSP-treated specimens

Figure 3 shows the three-dimensional surface morphology changes of the specimens before and after treatment under different laser shock peening (LSP) process parameters. As shown in Fig. 3a and b, the three-dimensional average surface roughness (Sa) of the untreated specimen is 0.472 μm, and the surface is relatively smooth. Fig. 3c, e, and g present the three-dimensional morphology of specimens after one LSP impact. Due to the Gaussian energy distribution of the laser spot, non-uniform plastic deformation occurs on the surface of 55SiMoVA steel, forming distinct peak–valley structures and micro-pits in localized areas. Taking the 4 J laser energy as an example (Fig. 3c), the surface roughness increases to 0.893 μm. With increasing laser energy, the surface roughness gradually rises, reaching a maximum of 1.578 μm under the 6 J condition (Fig. 3g). As shown in Fig. 3d, f, and h, with an increase in the number of LSP impacts, the depth of pits and the degree of plastic deformation on the specimen surface become more pronounced. When the number of impacts increases to two, the average surface roughness of the 4 J and 5 J

ISSN: 2688-8645

specimens rises to 1.490 μm and 1.646 μm, respectively, showing a significant increase compared to single-impact conditions, while the roughness of the 6 J specimen further increases to 2.206 μm.

Overall, the LSP process parameters have a significant influence on surface roughness: both increased laser energy and a higher number of impacts lead to a noticeable rise in roughness. This trend is consistent with the results reported by Li et al. [18], i.e., higher energy density and multiple impacts can induce more intense plastic deformation and a more complex microscopic pit morphology, thereby significantly increasing surface roughness. Specifically, the untreated specimen surface is relatively smooth; after single impacts at 4 J, 5 J, and 6 J, the roughness increases to varying degrees; while specimens subjected to two impacts show more pronounced pit features. This is highly consistent with the combined mechanism typical of the LSP process: "shockwave-induced high-strain-rate plastic deformation – surface material evaporation and redeposition – local surface reconstruction" [19]. It should be noted that under high-energy (6 J) conditions, the enhancement effect of increased energy on surface roughness is more prominent. This may not only result from stronger shockwave effects but also be related to partial melting or even vaporization of the protective layer under high energy, leading to further deterioration of the surface micro-morphology [20]. Under the 5 J double-impact condition, although roughness increases significantly, the overall level remains "moderate," which allows the formation of micro-pit structures on the surface that help retain and redistribute lubricating fluid while avoiding the adverse effects of excessive roughness under high energy. Such a "balancing effect" has also been noted in existing studies as beneficial for balancing wear resistance and friction stability [21]. Therefore, the LSP parameters of 5 J energy with two impacts show potential advantages in roughness control, which will be further reflected in the subsequent wear performance analysis.

## 3.2. Microhardness and Residual Stress Analysis

Fig. 4a, c, and e show the microhardness distribution of 55SiMoVA bearing steel after LSP treatment under different impact energies and numbers of impacts. The microhardness of the untreated specimen is about 646 HV, whereas after LSP treatment, the surface hardness increases significantly and gradually rises with higher impact energy and number of impacts. Under single-impact conditions, the surface hardness of specimens 1, 2, and 3 reaches 732 HV, 737 HV, and 745 HV, respectively, representing an increase of 14.4% to 16.4% compared to the untreated specimen. When the number of impacts increases to two, the hardness of specimens 4, 5, and 6 further rises to 739 HV, 751 HV, and 756 HV, with a maximum increase of 17%. Meanwhile, the depth of the hardened layer extends from 0.7 mm to 1.0 mm, indicating that the increased number of impacts not only enhances surface hardness but also expands the thickness of the strengthened layer. The main mechanism for the hardness increase can be attributed to the work-hardening effect caused by severe plastic deformation induced by the laser shockwave: the shockwave introduces a high density of dislocations and causes dislocation entanglement in the surface layer, thereby inhibiting dislocation slip and leading to significant hardening [22,23]. Furthermore, existing research has shown that LSP treatment can lead to grain refinement in the surface layer or even the formation of nanocrystalline structures, enhancing surface strength [24]. This strengthening effect typically exhibits a gradient distribution, with the highest hardness at the surface gradually decreasing with depth [25]. Fig. 4b, d, and f show the corresponding residual stress distributions. As can be more intuitively seen in Fig. b, which compares the surface residual stresses, the untreated specimen exhibits a surface residual compressive stress of about 23 MPa. The surface stress levels of LSP-treated specimens are significantly higher than those of the untreated specimen and tend to increase progressively with more impacts. Under single-impact conditions, the maximum residual compressive stresses for specimens 1, 2, and 3 are 746.8 MPa, 773.5 MPa, and

ISSN: 2688-8645

807.7 MPa, respectively. After two impacts, these values further increase to 805.1 MPa, 829.7 MPa, and 846.4 MPa, representing a maximum increase of over 823 MPa compared to the untreated state. Moreover, the depth of the residual compressive stress layer increases from 1 mm to 1.3 mm. When the impact parameters reach a certain threshold (e.g., 6 J double impact), the increase in residual compressive stress tends to saturate, and the strengthened layer approaches the material's limit; further increasing energy may not yield significant benefits and could even cause local damage [26]. In comparison, the specimen treated with 5 J impact energy and two impacts achieves a good balance in hardness, residual compressive stress, and strengthening layer thickness, demonstrating optimized overall performance.

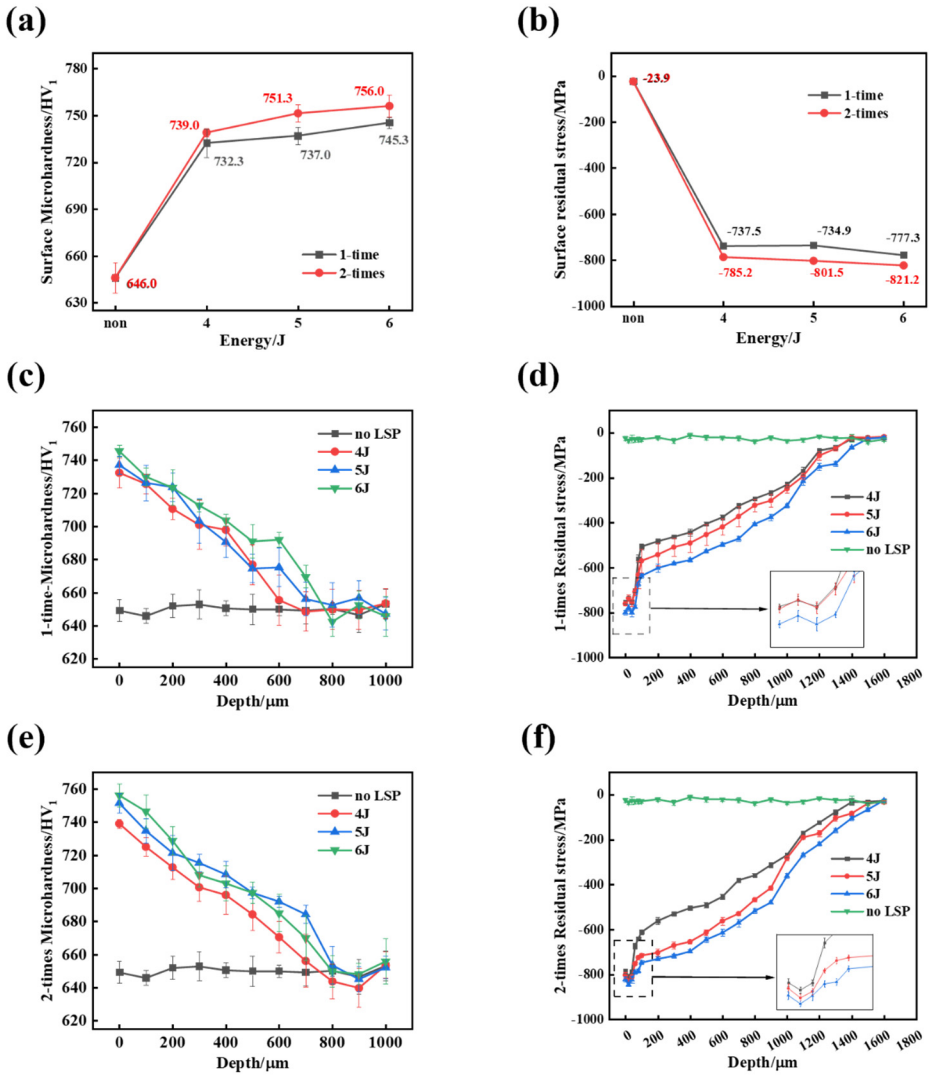


**Fig 4.** Surface and cross-sectional characterization under different LSP parameters: (a) surface microhardness; (b) surface residual stress; (c, e) cross-sectional microhardness; (d, f) cross-sectional residual stress

## 3.3. Friction and Wear

Figure 5 shows the variation of the coefficient of friction (COF) over time for 55SiMoVA bearing steel under different LSP parameters (energy: 4 J, 5 J, 6 J; number of impacts: 1, 2). All specimens undergo a distinct run-in stage at the beginning of friction, characterized by a gradual increase in COF; this is followed by a relatively stable stage, where the COF fluctuates slightly around a certain average value, reflecting the tribological performance of the material under steady-state wear conditions. In Fig. 5a, the COF curves of specimens treated with 4 J impact energy intersect with that of the untreated specimen, while the COF of the other

ISSN: 2688-8645

strengthened specimens is slightly higher than that of the untreated specimen. As shown in Fig. 5b, the run-in period of the untreated specimen exceeds 4000 s, whereas most specimens subjected to single impacts complete run-in within about 3000 s. Although the run-in stage is slightly shorter, specimens with single-impact strengthening exhibit larger fluctuations in COF during the initial run-in period, indicating that surface strengthening has not yet fully stabilized. Among specimens treated with two impacts (Fig. 5c, d), the friction curves generally show more stable trends. Specifically, the curves for specimens treated with 5 J and 6 J energy are very stable; however, the overall COF curve for the 5 J specimen lies below that of the untreated specimen, while the curve for the 6 J specimen lies above that of the 5 J specimen. This indicates that the specimen treated with 5 J energy and two impacts can maintain a lower and more stable frictional resistance after run-in, demonstrating the best frictional performance. Existing studies have shown that laser shock peening can improve friction performance and reduce fluctuations in the coefficient of friction by introducing compressive residual stresses and surface strengthening [27]. Combined with the results of this study, it can be seen that the 5 J energy with two impacts not only shortens the run-in stage but also maintains a lower and more stable COF during the steady-state friction stage, thereby enhancing overall wear resistance.

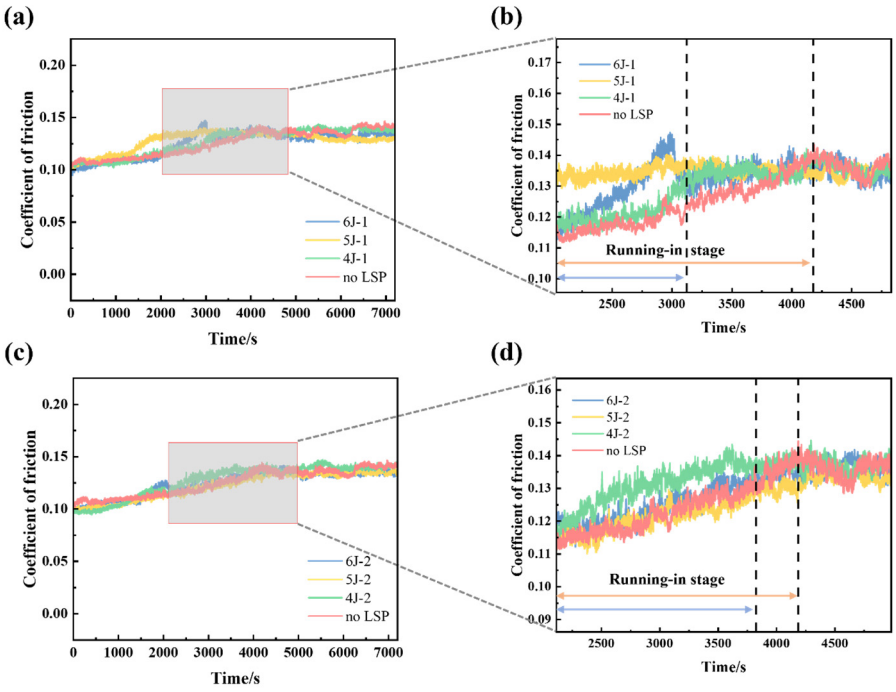


**Fig 5.** Friction coefficient curves of specimens under different LSP parameters: (a–b) comparison between untreated and single-impact specimens; (c–d) comparison between untreated and double-impact specimens

Figure 6 shows the wear scar morphology and the profiles of specified cross-sections of the wear scars for both untreated and strengthened specimens, further revealing the wear performance. The depth of the wear scar increases gradually from both sides towards the center, with the maximum wear depth occurring near the center of the scar. Slight protrusions can be observed within the wear scars of some specimens. This phenomenon may be related to the surface hardness gradient and residual stress distribution induced by Laser Shock Peening (LSP): LSP produces a high-hardness strengthened layer on the surface, while the underlying material has relatively lower hardness. During friction, localized plastic flow or rebound may occur in the softer regions, leading to the formation of central protrusions. Concurrently, the embedding of fine wear debris in the scar and uneven contact pressure distribution may also contribute to these local protrusions. Existing studies indicate that the hardness gradient,

ISSN: 2688-8645

residual stress field, and microstructural changes in LSP-treated materials can all lead to similar wear scar morphological features [28,29].

To quantitatively characterize the wear morphology, the wear morphology data from Figure 6a was selected to calculate the volumetric loss for each specimen, with the results shown in Figure 7a. The wear volume for the untreated specimen is 0.0134 $mm^3$. For the LSP-treated specimens: the wear volumes for single-impact specimens at 4J, 5J, and 6J impact energies are 0.0160 $mm^3$, 0.0171 $mm^3$, and 0.0133 $mm^3$, respectively; the wear volumes for double-impact specimens at the same energy levels are 0.0130 $mm^3$, 0.0107 $mm^3$, and 0.0114 $mm^3$, respectively. Compared to the untreated specimen, the parameter combination of 5 J impact energy with two impacts achieves the largest reduction in wear volume, up to 15%. However, the wear volume of some treated specimens is greater than that of the untreated specimen. This phenomenon may be related to excessive surface strengthening and changes in surface topography. High energy or multiple impacts may introduce localized microcracks or brittle zones on the surface, which are prone to spalling during friction, thereby increasing wear [30]. Additionally, LSP treatment may slightly increase surface roughness, where local protrusions can increase frictional contact stress and promote the formation of fine wear debris [31]. Therefore, although LSP generally improves material wear resistance, when processing parameters are too high or mismatched, an increase in wear volume may occur, necessitating a balance between the hardening effect and surface quality.

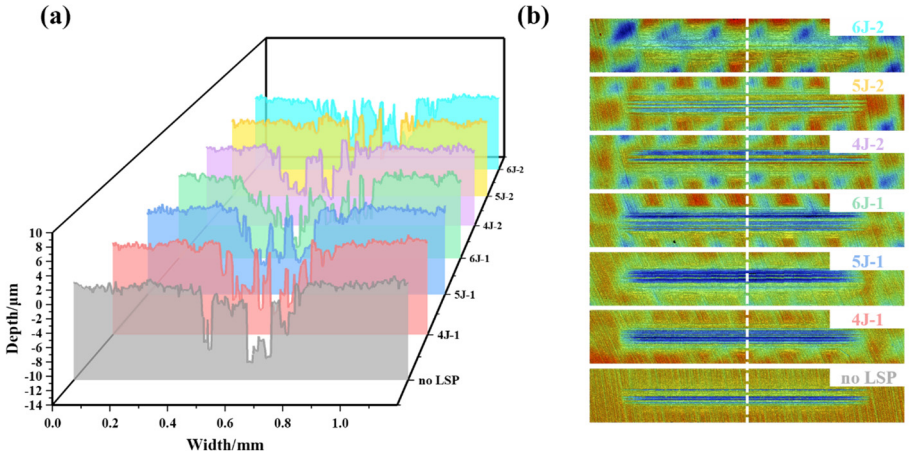


**Fig 6.** Cross-sectional profiles (a) and wear morphology (b) of worn surfaces under different LSP process parameters

Figures 7b-h present the scanning electron microscope (SEM) wear scar morphologies for each group of specimens. The surface of the untreated specimen (Specimen 0) shows numerous deep, groove-like features distributed along the sliding direction, with clear signs of typical abrasive plowing, reflecting insufficient material hardness. Under shear stress, severe plastic deformation occurs accompanied by material spalling, indicating poor wear resistance. The wear scar morphologies of Specimens 1, 2, and 4, treated with low energy or single impacts, show little difference from Specimen 0. Grooves remain deep, debris is evident, and some areas even exhibit microcracks or protrusions, suggesting that single impacts or low-energy treatments have limited effectiveness in improving wear resistance. In contrast, Specimens 5 and 6, treated with high-energy multiple impacts, exhibit much flatter wear scars with very few defects, showing only minor embedded abrasive particles or fine flaky spalling. This is primarily attributed to the multi-level plastic deformation and superimposed compressive residual stresses induced by multiple impacts, which create a denser surface microstructure with strong bonding to the substrate, effectively hindering microcrack propagation [32]. Comprehensive

ISSN: 2688-8645

SEM observation reveals that Specimens 3, 5, and 6 have the shallowest grooves and the least debris.

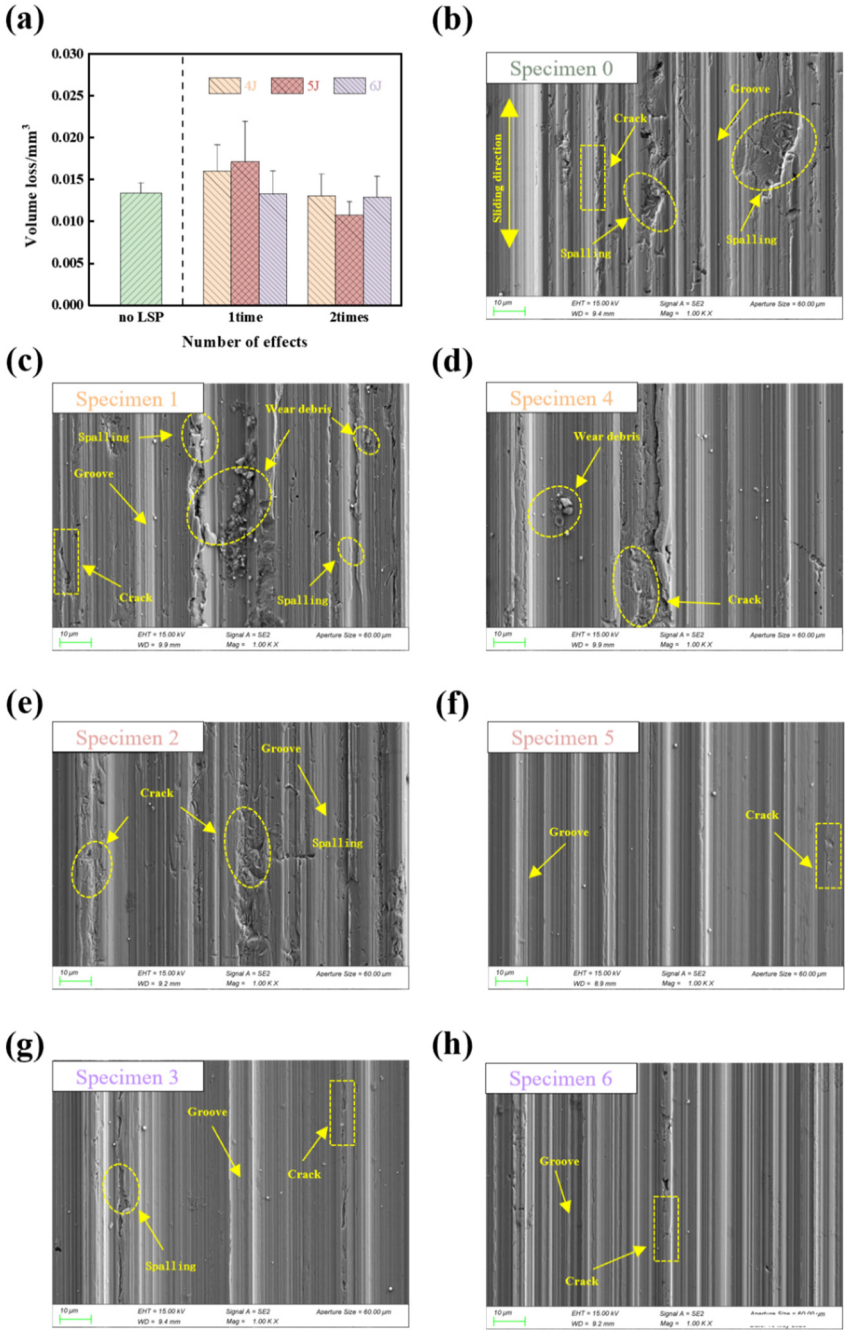


**Fig 7.** (a) Wear volume of specimens under different LSP parameters; (b–h) SEM images of worn surfaces under various LSP conditions

Among them, Specimen 5 exhibits the flattest wear scar with the fewest cracks, indicating that this parameter combination yields the best wear resistance improvement. Specimens 1, 2, and 4, along with other low-energy or single-impact specimens, still exhibit microcracks or protrusions, offering limited wear resistance advantages. Combining these findings with friction test results, the untreated and low-energy/single-impact specimens (0, 1, 2, 4) exhibited unstable friction processes, severe abrasive cutting, and susceptibility to local spalling and delamination wear, resulting in poor wear resistance. The friction surfaces of high-energy multiple-impact specimens were dominated by shallow grooves and fine spalling pits, appearing overall uniform without obvious signs of plastic tearing. This indicates that laser

ISSN: 2688-8645

shock peening effectively suppressed the plowing effect and the initiation and propagation of cracks, significantly mitigating surface erosion by abrasives [33]. These surface characteristics reduce the likelihood of abrasive wear and delamination wear, promote friction process stability, and thereby significantly enhance the wear resistance of 55SiMoVA bearing steel. Overall, specimens treated with multiple impacts or high energy exhibit excellent wear resistance in terms of both micromorphology and frictional behavior. Specimens treated with low energy or single impacts (1, 2, 4) show some improvement, but their wear resistance advantage is not significant. This validates the crucial synergistic role of optimizing laser energy and impact number for enhancing material wear resistance.

In summary, laser shock peening not only significantly alters the surface morphology of 55SiMoVA steel but also demonstrates remarkable advantages in grain refinement, the establishment of compressive residual stress, and the improvement of wear performance. However, its strengthening effect is highly sensitive to parameters, requiring careful control of energy and impact number to avoid potential damage caused by excessive roughness or residual stress concentration.

## 4. Summary

This study systematically analyzed the changes in the frictional performance of 55SiMoVA bearing steel subjected to Laser Shock Peening (LSP) treatment. By employing parameter combinations of three laser energy levels (4J, 5J, 6J) and two impact numbers (1, 2), the effects of LSP treatment power and impact number on the material's surface strengthening and its friction and wear behavior were comprehensively evaluated. Based on the experimental results, the following conclusions can be drawn:

(1) LSP process parameters significantly affect surface roughness. The Sa value of the untreated specimen is 0.472 μm, increasing by approximately 367% to a maximum of 2.206 μm under the 6 J double-impact condition.

(2) LSP treatment significantly enhances the mechanical properties of 55SiMoVA bearing steel. It introduces beneficial compressive residual stress in the near-surface region, with a maximum value reaching -804.3 MPa. Microhardness is also markedly increased, with surface hardness reaching 756 HV, representing a 17% improvement over the untreated specimen.

(3) LSP shortens the run-in period. The run-in period for the untreated specimen is about 4000 s, reduced by approximately 25% to about 3000 s for single-impact specimens. The specimen treated with 5 J energy and two impacts maintains the lowest and most stable COF curve during the steady-state stage and achieves a reduction in wear volume of about 15%, demonstrating the best friction and wear performance. However, specimens treated with low energy and single impacts showed a slight increase in wear volume, indicating the need to balance strengthening effects with surface quality.

(4) SEM microanalysis shows that untreated, low-energy, and single-impact specimens exhibit deep grooves, numerous cracks, unstable friction, and poor wear resistance. High-energy multiple-impact specimens have a dense surface layer, shallow grooves, and few cracks. The combination of compressive residual stress and hardness strengthening effectively inhibits microcrack propagation, with the 5 J double-impact specimen showing the best surface flatness. Localized microcracks or protrusions are still visible in some high-energy treated specimens, suggesting that excessively high energy may cause micro-damage to the surface layer. Therefore, optimizing LSP parameters requires balancing the strengthening effect with material integrity.

## Acknowledgments

Supported by Sichuan Science and Technology Program (No.2024NSFSC2021).

## References

[1] Wang J T, Tan C F, Wang L P, et al. Screw drilling of positive displacement motors failure analysis and improve the life of measures to discuss[J]. West. Exp. Eng. China, 2010, 22: 57-59.

[2] Zhang J, Liang Z, Han C. Failure analysis and finite element simulation of key components of PDM[J]. Engineering Failure Analysis, 2014, 45: 15-25.

[3] Yu X, Shi G, Gao W, et al. Effects of differently shaped textures on the tribological properties of static and dynamic pressure thrust bearings and multiobjective optimization[J]. Industrial Lubrication and Tribology, 2024, 76(6): 769-787.

[4] Han C J, Zhang J, Liang Z. Design and analysis of thrust hollow tapered roller bearing for screw drilling tools[J]. Journal of China University of Petroleum (Natural Science Edition), 2014, 38(3): 123-128.

[5] Sexton T N, Cooley C H. Polycrystalline diamond thrust bearings for down-hole oil and gas drilling tools[J]. Wear, 2009, 267(5-8): 1041-1045.

[6] Zhang X, Yu Z. Effect of laser shock processing on fatigue life of fastener hole[J]. Transactions of Nonferrous Metals Society of China, 2014, 24(4): 969-974.

[7] Luo S, Nie X, Zhou L, et al. High cycle fatigue performance in laser shock peened TC4 titanium alloys subjected to foreign object damage[J]. Journal of Materials Engineering and Performance, 2018, 27(3): 1466-1474.

[8] Trdan U, Skarba M, Porro J A, et al. Application of massive laser shock processing for improvement of mechanical and tribological properties[J]. Surface and Coatings Technology, 2018, 342: 1-11.

[9] Zhang Y, Guo W, Shi J, et al. Improved rotating bending fatigue performance of laser directed energy deposited Ti6Al4V alloys by laser shock peening[J]. Journal of Alloys and Compounds, 2024, 980: 173664.

[10] Zabeen S, Langer K, Fitzpatrick M E. Effect of alloy temper on surface modification of aluminium 2624 by laser shock peening[J]. Surface and Coatings Technology, 2018, 347: 123-135.

[11] Rajan S S, Manivasagam G, Ranganathan M, et al. Influence of laser peening without coating on microstructure and fatigue limit of Ti-15V-3Al-3Cr-3Sn[J]. Optics & Laser Technology, 2019, 111: 481-488.

[12] Ge M Z, Xiang J Y, Tang Y, et al. Wear behavior of Mg-3Al-1Zn alloy subjected to laser shock peening[J]. Surface and Coatings Technology, 2018, 337: 501-509.

[13] Zhou J, Sun Y, Huang S, et al. Effect of laser peening on friction and wear behavior of medical Ti6Al4V alloy[J]. Optics & Laser Technology, 2019, 109: 263-269.

[14] Park J, Yeo I, Jang I, et al. Improvement of friction characteristics of cast aluminum-silicon alloy by laser shock peening[J]. Journal of Materials Processing Technology, 2019, 266: 283-291.

[15] Nataraj M V, Swaroop S. Effects of power density on residual stress and microstructural behavior of Ti-2.5 Cu alloy by laser shock peening without coating[J]. Vacuum, 2023, 213: 112078.

[16] Liu L, Lin Y, Peng L, et al. Progress in microstructure design and control of high-hardness Fe-based alloy coatings via laser cladding[J]. Coatings, 2024, 14(11): 1351.

[17] Muthukumaran G, Rai A K, Gautam J, et al. A study on effect of multiple laser shock peening on microstructure, residual stress, and mechanical strength of 2.5 Ni-Cr-Mo (EN25) low-alloy steel[J]. Journal of Materials Engineering and Performance, 2023, 32(10): 4361-4375.

[18] Li Y, Qiao L, Dang X, et al. Surface Integrity Evolution and Fretting Wear Improvement of DD6 Single-Crystal Superalloy via Laser Shock Peening and Laser Shock Peening Without Coating[J]. Metals, 2025, 15(8): 889.

[19] Zhang P, Gao Y R, Wang X Z, et al. Mechanism of water-guided laser strengthening on surface integrity and fatigue behavior of 2519A aluminum alloy (Invited)[J]. Chinese Journal of Lasers, 2025, 52(14): 1402123-1–1402123-12.

[20] Li B, Wang Z, Kong M, et al. Tailoring the surface integrity and wear resistance of WE43 Mg alloy by warm laser shock peening[J]. Journal of Materials Research and Technology, 2025, 35: 1504-1518.

[21] Sarukasan D, Thirumavalavan K. Investigations of surface characteristics on AA5083 alloy with dual treatment[J]. Surface Engineering, 2025, 41(2): 279-292.

[22] Sun Y, Yu X, Liu W, et al. Effect of laser shock peening on wear resistance of M50 steel[J]. Materials Science and Technology, 2024, 40(13): 969-979.

[23] Yang Q T, Zhang Y K, Chi Y Q, et al. Effect of laser shock peening on microstructure and properties of E690 steel for marine engineering[J]. 2023.

[24] Tang Z, Hou Z, Du H, et al. Effects of laser shock peening on the surface integrity and fatigue properties of 34CrNiMo6 steel[J]. Proceedings of the Institution of Mechanical Engineers, Part B: Journal of Engineering Manufacture, 2025: 09544054241309163.

[25] Xiong Y, Zhou T, Chen Z, et al. Laser shock peening rounds influencing microstructural and mechanical properties of 300M steel[J]. Materials Science and Technology, 2023, 39(16): 2217-2229.

[26] Li N, Wang Q, Niu W, et al. Effects of multiple laser shock peening impacts on microstructure and wear performance of wire-based laser directed energy deposition 17-4PH stainless steel[J]. Journal of Materials Research and Technology, 2023, 25: 3222-3227.

[27] Sarukasan D, Thirumavalavan K. Influencing laser shock peening treatment of the mechanical, tribological, corrosion, and microstructural characteristics on AA5052 alloy[J]. Surface Engineering, 2024, 40(9-10): 945-966.

[28] Liu Q, Chu S, Zhang X, et al. Laser shock processing of titanium alloys: A critical review on the microstructure evolution and enhanced engineering performance[J]. Journal of Materials Science & Technology, 2025, 209: 262-291.

[29] Yong W, Xiaoyu P A N, Xibin W, et al. Influence of laser shock peening on surface integrity and tensile property of high strength low alloy steel[J]. Chinese Journal of Aeronautics, 2021, 34(6): 199-208.

[30] Yang S, Zhang M, Yu P, et al. Effect of laser shock peening overlap rate on microstructure and wear resistance of M50 steel[J]. Optics & Laser Technology, 2025, 184: 112548.

[31] He T, Gong Z, Liu Z, et al. Effect of Laser Shock Peening Impact Numbers on Microstructure and Tribological Characteristics of GCr15 Steel[J]. Journal of Materials Engineering and Performance, 2025, 34(12): 10891-10905.

[32] Madapana D, Ramadas H, Nath A K, et al. Studies on laser shock peening on nanomechanical and mechano-chemical properties of titanium alloy (Ti6Al4V)[J]. Jom, 2023, 75(1): 109-119.

[33] Feng A, Xu G, Chen C, et al. Surface characteristics and wear resistance of GCr15 bearing steel by cryogenic treatment-laser peening[J]. Applied Physics A, 2022, 128(10): 921.